Complex Metabolic Oscillations in Plants Forced by Harmonic Irradiance

Ladislav Nedbal and Vítězslav Březina
Photosynthesis Research Center, Laboratory of Applied Photobiology and Bio-Imaging, Institute of Landscape Ecology CAS and Institute of Physical Biology, University of S. Bohemia, Zámek 136, CZ-37333 Nové Hrady, Czech Republic

ABSTRACT Plants exposed to harmonically modulated irradiance, $\approx 1 + \cos(\omega t)$, exhibit a complex periodic pattern of chlorophyll fluorescence emission that can be deconvoluted into a steady-state component, a component that is modulated with the frequency of the irradiance (ω), and into at least two upper harmonic components (2ω and 3ω). A model is proposed that accounts for the upper harmonics in fluorescence emission by nonlinear negative feedback regulation of photosynthesis. In contrast to simpler linear models, the model predicts that the steady-state fluorescence component will depend on the frequency of light modulation, and that amplitudes of all fluorescence components will exhibit resonance peak(s) when the irradiance frequency is tuned to an internal frequency of a regulatory component. The experiments confirmed that the upper harmonic components appear and exhibit distinct resonant peaks. The frequency of autonomous oscillations observed earlier upon an abrupt increase in CO_2 concentration corresponds to the sharpest of the resonant peaks of the forced oscillations. We propose that the underlying principles are general for a wide spectrum of negative-feedback regulatory mechanisms. The analysis by forced harmonic oscillations will enable us to examine internal dynamics of regulatory processes that have not been accessible to noninvasive fluorescence monitoring to date.

INTRODUCTION

Photosynthesis is a highly adaptive process, allowing plants to harvest and utilize the energy of light in a very dynamic environment. Phytoplankton moving with ocean waves or plants exposed to sunflecks in a wind-moved canopy can cope with irradiance oscillating between levels in which photosynthesis barely compensates for respiration to levels in which they reach or exceed their maximum photosynthetic capacity. The photosynthetic machinery rapidly adapts to external conditions to avoid harmful disharmony between energy influx and capacity of the plant to utilize the absorbed energy. State transitions balancing the distribution of excitation energy between the two photosystems and nonphotochemical quenching are well-known examples of molecular regulation maintaining the homeostasis of photosynthetic processes by a negative feedback control of the excitation energy input (Demmig-Adams and Adams, 1992; Fork and Satoh, 1991; Horton and Ruban, 1992).

Here, we investigate the regulation in plants by studying the chlorophyll fluorescence response to harmonically modulated irradiance. We propose that modulation frequency may be tuned to resonate with internal regulatory mechanisms ranging from nonphotochemical quenching to circadian rhythms. For practical reasons, we are focusing here only on a timescale of tens of seconds, but the system analysis of the photosynthetic negative feedback regulations and the proposed method should be general regardless of particular molecular mechanism and timescale.

Submitted January 7, 2002, and accepted for publication May 24, 2002.

Address reprint requests to Ladislav Nedbal, Laboratory of Applied Photobiology and Bio-Imaging, Institute of Landscape Ecology, Zámek 136, CZ-37333 Nové Hrady, Czech Republic. Tel.: ++420-335-361111; Fax: ++420-335-361231; E-mail: nedbal@greentech.cz.

0006-3495/02/10/2180/10 $2.00

The molecular basis of the key structures of both the light and dark phases of photosynthesis is well understood (Leegood et al., 2000; Ort and Yocum, 1996). Membrane-bound photosystem II uses light energy to oxidize water on the lumenal side of the thylakoid and to deliver the extracted electrons, through the mobile plastoquinone pool, to the cytochrome b_6/f complex. The cytochrome b_6/f is oxidized via plastocyanine (or via soluble cytochromes) by the light-driven charge separation in photosystem I. The electrons subsequently released by photosystem I on the stromal side of the thylakoid membrane reduce $NADP^+$ to NADPH. The light-driven reactions are oriented in the membrane to accumulate protons on the lumenal side of the membrane and the reducing equivalents on the stromal side of the membrane. The difference of electrochemical potential between the two sides of the thylakoid membrane is used by membrane-bound ATPase to phosphorylate ADP to ATP. The reducing power of NADPH and the chemical energy of ATP are used in the Calvin cycle to turn inorganic carbon dioxide into molecules of glucose that can be used in respiration, stored in starch, converted to cellulose of cell walls, or transformed into a variety of other vital organic compounds.

The rate at which photosynthetically generated ATP and NADPH are used by the Calvin cycle is reflected by the redox state of the plastoquinone pool that is one of the key elements determining the fluorescence quantum yield. The more efficiently ATP and NADPH are used, the higher the photochemical quenching of chlorophyll fluorescence and the lower the fluorescence emission yield. Thus, fluorescence emission can serve as a quantitative noninvasive intrinsic probe of photosynthetic electron transport (Genty et al., 1989; Weis and Berry, 1987).

The complex network of interacting and regulating components of plant photosynthesis can be approached by studying its fluorescence response to a variable energy

input. Even in case in which we know little about the molecular nature of the regulation, significant conclusions can be made about the dynamic properties of the system (Ljung, 1991). The system-level approach to living organisms may also have a significant advantage over analytical investigation on the organelle or molecular level because it can reveal structural modules, interactions, and modes of operation that lend the complex system robustness to uncertain and highly dynamic environments (Kitano, 2001). These features constitute a base for a significant and often dominant fraction of structural modules of any complex system (Csete and Doyle, 2002). The potential of system-level analysis of forced (Demin et al., 1999) and autonomous (Reijenga et al., 2002) oscillations has already been widely utilized in analyzing diverse biological systems, reviewed in Hess (2000). The applications in photosynthesis are still scarce despite the unique opportunity given by the fully controllable energy input of plant bioenergetics. The earlier research of periodic phenomena in photosynthesis has to date been mostly limited to autonomous oscillations caused by a stepwise change in external conditions (e.g., Giersch, 1994; Laisk and Eichelmann, 1989; Rovers and Giersch, 1995; Ryde-Pettersson, 1992; Walker, 1992).

Here, we use harmonically modulated light of a variable frequency as an input and fluorescence emission as the output conveying the information about internal dynamic properties of the system. The harmonic forcing leads to a form of differential equations describing the system dynamics that can often be solved analytically providing valuable insight into the observed phenomena.

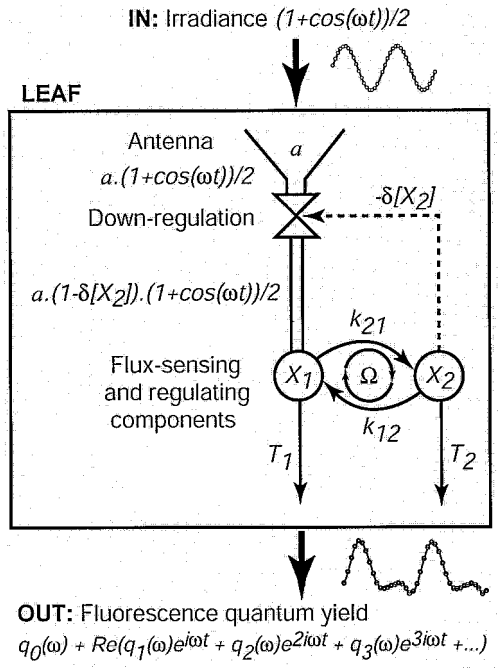

FIGURE 1 System-level presentation of model components. Leaf symbolized by the box in the middle of the scheme was exposed to harmonically modulated irradiance. The chlorophyll fluorescence emission was measured as a system output and deconvoluted into steady-state, fundamental (ω), and two upper harmonic components (2ω, 3ω). The oscillatory system behavior was modeled mathematically using two flux-sensing and regulating components X_1 and X_2. The component X_2 is proposed to down-regulate the energy influx by a regulatory interaction δ (*dashed line*).

THEORETICAL METHODS AND MODELS

The change in concentration of one reactant $d[X_j]/dt$ can be related to the instantaneous concentrations of all reactants $[X_{i=1,N}]$ in a set of N first-order differential equations (N is the number of interacting components). Complex nonlinear models (Laisk and Eichelmann, 1989) can be solved only by numerical methods, whereas in a frequently used linear approximation (e.g., Ryde-Pettersson, 1990), simpler models lead to a set of linear differential equations:

$$d[X_j]/dt = \sum_{k=1}^{N} a_{jk}[X_k] \qquad (1)$$

The complexity of plant photosynthetic reactions is also frequently reduced to a small number of components interacting on the timescale relevant to a given experimental situation (Rovers and Giersch, 1995). With a kinetic scheme including only two reactants, up to 16 combinations of rate constants were identified that led to a prediction of oscillatory/resonance behavior (Ryde-Pettersson, 1990). The mathematical description of such a model is reduced to a set of two linear, first-order equations that can be solved analytically. The solution takes the form of damped oscillations:

$$[X_j](t) = [X_j](\infty) + A_j e^{-\sigma t}\cos(\Omega t + \varphi_j) \qquad (2)$$

with the first term $[X_j](\infty)$ representing a steady-state equilibrium concentration, A_j representing oscillation amplitude, σ representing damping rate constant, Ω representing oscillation frequency, and φ representing oscillation phase. Damped oscillations of photosynthetic activity are observed experimentally, and several mathematical models yielding results similar to Eq. 2 were used to link the experiment with relevant photosynthetic rate constants (Buschmann and Gradmann, 1997; Fridlyand, 1998; Giersch, 1994; Laisk and Eichelmann, 1989; Ryde-Pettersson, 1992).

Here, we show that a more advanced nonlinear model is needed to account for the experimental results from forced oscillations (Fig. 1). Let us assume that a reactant X_1 is generated with a rate proportional to the incident harmonic irradiance $(1 + \cos(\omega t))/2$ and to the effective antenna size a (Fig. 1). The energy input is further modulated through a negative feedback interaction δ by the concentration of a second flux-sensing and regulating reactant $[X_2]$. The well-established mechanisms of nonphotochemical quenching of chlorophyll fluorescence and of state-transitions are exam-

ples of processes that can be modeled by the interaction δ as proposed in Fig. 1 (Demmig-Adams and Adams, 1992; Fork and Satoh, 1991; Horton and Ruban, 1992). The kinetics of the reactants can then be described by a set of two differential equations, Eqs. 3 a and b, that are related to Eq. 1 but are augmented by a nonlinear term $(1 - \delta[X_2])(1 + \cos(\omega t))/2$ representing the negative feedback regulation of the harmonic forcing:

$$d[X_1]/dt = -[X_1]/T_1 + k_{12}[X_2] + a(1 - \delta[X_2])(1 + \cos(\omega t))/2 \quad (3a)$$

$$d[X_2]/dt = k_{21}[X_1] - [X_2]/T_2 \quad (3b)$$

The concentration of the reactant $[X_1]$ can be expressed using Eq. 3b and substituted into Eq. 3a so that a single second-order differential equation for the regulating reactant $[X_2]$ is obtained:

$$\frac{d^2[X_2]}{dt^2} + \left(\frac{1}{T_1} + \frac{1}{T_2}\right)\frac{d[X_2]}{dt} + \left(\frac{1}{T_1}\frac{1}{T_2} - k_{21}k_{12}\right)[X_2] = k_{21}a(1 - \delta[X_2])(1 + \cos(\omega t))/2 \quad (4)$$

Equation 4 is of an identical form to an equation that is widely used and often solved to describe mechanical vibrations or resonance of electric charge Q in an electronic circuit consisting of serially wired inductance L, resistance R, and capacitance C:

$$\frac{d^2Q}{dt^2} + \frac{R}{L}\frac{dQ}{dt} + \frac{1}{LC}Q = \frac{1}{L}(1 - \delta Q)(1 + \cos(\omega t))/2 \quad (5)$$

The harmonic forcing $\cos(\omega t)$ that is usually used in electronics is replaced in Eq. 5 by a driving force $(1 - \delta Q)(1 + \cos(\omega t))/2$ including the negative feedback regulation through δ.

Using existing literature (Dettman, 1961), the homology between Eqs. 4 and 5 helps to get results for resonating photosynthetic apparatus without extensive mathematical exercise.

To further simplify the mathematics, Eq. 5 can be rewritten into a more phenomenological form:

$$\frac{d^2Q}{dt^2} + 2\sigma\frac{dQ}{dt} + (\sigma^2 + \Omega^2)Q = (1 - \delta Q)(1 + \cos(\omega t))/2 \quad (6)$$

where $\sigma = R/2L$ represents the inverse time constant at which oscillations are damped and $\Omega = i\sqrt{1/LC - R^2/4L^2}$ is the frequency at which autonomous oscillations elicited by stepwise input occur. In the case of photosynthesis, this can be the frequency of autonomous oscillations occurring in response to abrupt changes in CO_2 concentration, whereas σ is the inverse time-constant of the damping of these oscillations (reviewed in Giersch, 1994; Walker, 1992). Homology with Eq. 4 shows that the damping constant σ is proportional to the inverse lifetimes of the components X_1 and X_2 in Fig. 1 ($2\sigma = 1/T_1 + 1/T_2$). Various combinations of rate constants in simple systems of reactants that lead to autonomous oscillations are discussed in Ryde-Pettersson (1990).

For a negligible regulation ($\delta \approx 0$), Eq. 6 is linear and can be solved analytically. In a steady state ($t \gg 1/\sigma$), the solution of Eq. 6 is a harmonic function with a frequency equal to the input modulation frequency ω and with a steady-state mean value q_0 that is independent of modulation frequency:

$$Q(t) = q_0 + q_1(\omega)e^{i\omega t} + \overline{q_1(\omega)}e^{-i\omega t} \quad (7)$$

In the case of an effective regulation ($\delta \neq 0$), Eq. 6 includes higher harmonics of the modulation frequency:

$$Q(t) = q_0(\omega) + \sum_{n=1}^{\infty}(q_n(\omega)e^{in\omega t} + \overline{q_n(\omega)}e^{-in\omega t}) \quad (8)$$

The occurrence of higher harmonics in Eq. 8 results from nonlinearity of the product $\delta \cdot Q \cdot \cos(\omega t)$ on the right-hand side in Eq. 6:

$$\delta Q\cos(\omega t) = \delta(q_0(\omega) + \sum_{n=1}^{\infty}(q_n(\omega)e^{in\omega t} + \overline{q_n(\omega)}e^{-in\omega t})) \cdot (e^{i\omega t} + e^{-i\omega t})/2 \quad (9)$$

The nonlinear factor (Eq. 9) couples components oscillating with frequency $n\omega$ to components oscillating with frequencies $(n + 1)\omega$ and $(n - 1)\omega$ causing upper harmonics to contribute to Q kinetics and, in homologous biological systems, upper harmonics to occur in the fluorescent signal.

Assuming that the regulatory interaction is small ($0 < \delta \ll 1$), the harmonics higher than $e^{\pm 2i\omega t}$ can be neglected in Eq. 8. Then the coefficients q_0, q_1, and q_2 can be determined by combining Eqs. 6 and 8 and by comparing the factors that are constant in time separate from those that are changing as $e^{i\omega t}$ and $e^{2i\omega t}$, respectively. The steady-state mean q_0 is frequency-dependent through q_1:

$$q_0(\omega) = \frac{1 - \delta(q_1(\omega) + \overline{q_1(\omega)})/2}{2(\Omega^2 + \sigma^2 + \delta/2)} \quad (10)$$

The coefficient q_1 representing the component oscillating at the same frequency as the harmonic input is frequency-dependent explicitly with a clear resonance character:

$$q_1(\omega) = \tfrac{1}{4}(1 - \delta(q_0 + q_2)) \times \frac{((\Omega^2 + \sigma^2 + \delta/2) - \omega^2) - i(2\sigma\omega)}{((\Omega^2 + \sigma^2 + \delta/2) - \omega^2)^2 + (2\sigma\omega)^2} \quad (11)$$

The coefficient q_2, representing the first upper harmonic component $e^{2i\omega t}$, is proportional to the regulatory interaction δ:

$$q_2(\omega) = -\frac{\delta}{4}(q_1 + q_3)) \times \frac{((\Omega^2 + \sigma^2 + \delta/2) - (2\omega)^2) - i(4\sigma\omega)}{((\Omega^2 + \sigma^2 + \delta/2) - (2\omega)^2)^2 + (4\sigma\omega)^2} \quad (12)$$

In the first-order approximation for a small δ, the coefficient q_3 in Eq. 12 can be neglected because it is proportional to at least δ^2. The first upper harmonics q_2, however, cannot be neglected for any non-zero regulatory interaction δ because it is coupled in Eqs. 11 and 12 to the fundamental frequency coefficient q_1. Thus, the higher harmonic component always occurs when the regulatory interaction δ cannot be neglected. The effective regulatory interaction δ is also manifested by the frequency-dependence of the steady-state mean value q_0 shown in Eq. 10.

We propose that the redox state of flux-sensing and regulating component X_2 in Fig. 1 (Q in Eqs. 5–9) is reflected through a negative-feedback regulation δ in the quenching of chlorophyll fluorescence emission. The experiments presented here were designed to verify the model, namely to determine whether the upper harmonic components (q_1, q_2) are found in the variable part of the fluorescence emission and whether amplitude of the steady-state fluorescence component (q_0) depends on frequency of the harmonically modulated irradiance. If confirmed, these higher-order effects indicate nonlinear negative feedback regulation of photosynthesis.

MATERIALS AND METHODS

Plant material

The African violet *Saintpaulia brevipilosa* was grown in the laboratory at room temperature and irradiance. Tobacco plants (*Nicotiana tabacum*) were also potted in soil and grown in a Sanyo growth chamber with a 12 h/12 h day/night cycle with 400 μmol(photons)·m^{-2}·s^{-1} day irradiance. The leaf being subjected to harmonic irradiance remained attached to the plant, and only its position was fixed horizontally by a plastic wire grid pressing it gently toward an aluminum plate that was temperature-controlled by a Peltier cell (ThermoRegulator, Photon Systems Instruments, Ltd., Brno, Czech Republic, http://www.psi.cz). Together with the investigated leaf a large part of the plant was also exposed to the harmonic irradiance, so that no steep gradient in the light environment was present during the exposure. The experiments were repeated five times with different leaves.

The herbicide DCMU (3-(3′,4′-dichlorophenyl)-1,1-dimethylurea), 2 mM solution in 1% dimethylsulfoxide in water, was applied to the surface of one leaf of an African violet. After a week the herbicide diffused to the neighboring leaves, where it was localized close to the stem and large veins. The herbicide localization within the leaf tissue was checked by imaging of fluorescence in weak light.

Light sources and imaging of fluorescence

Images of fluorescent emission were captured as described in Nedbal et al. (2000) using a FluorCam kinetic imaging fluorometer (Photon Systems Instruments, Ltd.). The objective lens of the CCD camera was ~7 cm perpendicular to the leaf surface. The measuring flashes were generated in two panels of orange light-emitting diodes (HLMP-EH08, Agilent Technologies, Palo Alto, CA) that are a standard component of the FluorCam system. There were always 20 measuring flashes generating 20 images of fluorescence emission captured in each period of the harmonically modulated actinic light. The measuring flashes were 10 μs long and had no detectable actinic effect.

The actinic light was generated in the same panels of light-emitting diodes using a modified FluorCam control unit and power supply. The instrument was modified to generate electric current for light-emitting diodes that is linearly modulated by harmonic voltage delivered by an external digital function generator. The generator was triggered externally by a TTL pulse from the FluorCam so that each protocol was executed with modulated light of the same phase. The actinic light was modulated with periods ranging from 3 s to 135 s.

The images representing instantaneous fluorescence quantum yield mapped over the leaf surface were always captured during 13 periods of the harmonic irradiance modulation. Dynamic equilibrium was established after 10 periods so that very similar stationary kinetic patterns were obtained for the 10th, 11th, and 12th periods. These periods were used for numeric analysis.

Next to the plant leaf, an inert laboratory-made fluorescent standard (plastic sheet with immobilized Nile blue laser dye) was placed within the viewing angle of the camera. The fluorescent signal of the dye was used to eliminate, by normalization, small (~±1.2%) fluctuations in the power of the measuring flashes that were caused by an interaction between actinic and measuring operation regimes of the light-emitting diodes. The same fluorescent standard was used to accurately record the amplitude and phase of the incident harmonic irradiance. The absolute irradiance at the limiting levels was determined by a Licor quantum sensor. The actinic irradiance was changing from 15 μmol(photons)·m^{-2}·s^{-1} at the minimum to 145 μmol(photons)·m^{-2}·s^{-1} at the maximum of the harmonic wave in most of the experiments.

Data analysis

Fourier analysis of the kinetics in individual pixels of the fluorescence images shown in Fig. 3 was performed using the FFT tool of the Recognita software (Photon Systems Instruments, Ltd.). Simple transients of fluorescence were kinetically analyzed by MatLab software (MathWorks, Inc., Natick, MA).

RESULTS

Upper harmonic components in chlorophyll fluorescence emission are a hallmark of forced oscillations in plants

Tobacco leaves were exposed to harmonically modulated irradiance with periods of 60 and 80 s (thin line in the upper panels of Fig. 2). The emitted fluorescence (closed large circles in the upper panels of Fig. 2) clearly deviates from the single-frequency harmonic pattern predicted by linear models for a zero negative-feedback interaction (Eq. 7). Fourier analysis (not shown) reveals that the kinetics consists, in addition to a component of the fundamental frequency ($\omega = 2\pi/60$ s^{-1} and $2\pi/80$ s^{-1}, respectively), of at least two upper harmonic components (2ω, 3ω). The result of the Fourier analysis is confirmed by the fit of the experimental data by a periodic function constructed from three harmonic components ($F(t) \approx q_0 + q_1 \cdot \cos(\omega t + \varphi_1) + q_2 \cdot \cos(2\omega t + \varphi_2) + q_3 \cdot \cos(3\omega t + \varphi_3)$) that is shown by small

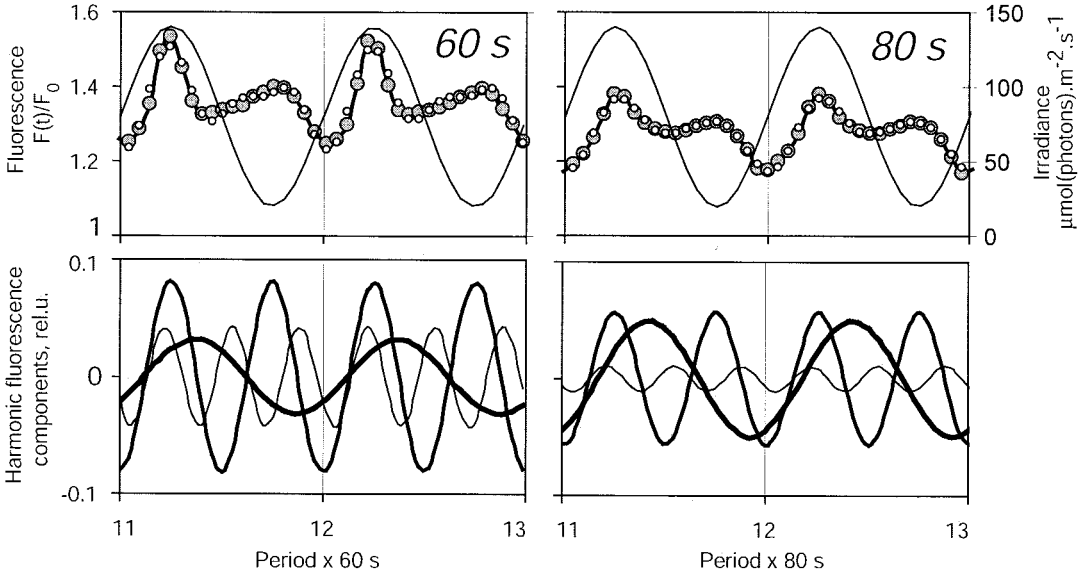

FIGURE 2 Leaf of tobacco was exposed to harmonically modulated light of two periods: 60 s (*left*) and 80 s (*right*); with irradiance oscillating between 15 and 145 μmol(photons)$\cdot$m$^{-2}\cdot$s^{-1} (*thin line in the top panels*). The normalized chlorophyll fluorescence yield was measured (*large closed circles in top panels*) and deconvoluted into three harmonic components (*bottom panels*). Each data point represents one image of emitted fluorescence. The small white dots in the top panels represent fit of the data by a combination of steady-state and of fundamental ($\omega = 2\pi/60$ s^{-1} and $2\pi/80$ s^{-1}, respectively), and two upper harmonic components (2ω and 3ω). The three harmonic components are shown in the bottom panel: thick line for the fundamental component (ω), medium line for the first upper harmonic component (2ω), and thin line for the second upper harmonic component (3ω).

open circles in the upper panels of Fig. 2. The individual harmonic components revealed by the numeric fitting of the fluorescence kinetics are shown in the bottom panels of Fig. 2. The fluorescence transient elicited by irradiance of a 60-s period consists of upper harmonic components with significantly larger amplitudes (Fig. 2, *bottom left*) than those with an 80-s period (Fig. 2, *bottom right*). The presence of the upper harmonic components in fluorescence emission confirms the prediction of the nonlinear model with an active negative-feedback regulation (Eq. 12).

The Fourier analysis was performed in all pixels of the leaf image using a proportional fraction of the total 120,000 transients captured by the camera. Fig. 3 demonstrates a qualitatively uniform fluorescence response to a 60-s harmonic irradiance in another tobacco leaf. The uneven surface of the tobacco leaf was intercepting more of the incident measuring and actinic irradiance in the right-hand half of the leaf that, consequently, exhibited higher fluorescent emission both at the maximum of the harmonic actinic irradiance (F1, Fig. 3 *A*) and when the irradiance was at its minimum (F0, Fig. 3 *B*). The normalized harmonic variability of the fluorescence yield (F1 − F0)/F1 shown in Fig. 3 *C* was, however, rather uniform over the entire leaf surface.

Amplitudes of three harmonic components and their phase shifts relative to the harmonic modulation of the actinic light (see bottom panels in Fig. 2) were determined for all camera pixels used for imaging fluorescence emission of the leaf. For each harmonic component a leaf image was constructed indicating the phase of the component by color and amplitude by brightness. Fig. 3 *D* represents such an analysis for the fundamental harmonic component of the fluorescent emission. Red indicates that the fluorescent response was slightly plus-shifted in time relative to the irradiance input (a small minus-shift would be blue and a maximum shift by a half-period would be green). Amplitude of the fundamental component ($\omega = 2\pi/60$ s^{-1}) was highest, on an absolute scale, in the right-hand half of the leaf that was exposed to high light and smallest in the least irradiated segments of the left-hand half of the leaf and in the veins.

Similar features were found also for the first upper harmonics ($\omega = 2.2\pi/60$ s^{-1}) presented in Fig. 3 *E*. Here, the contrast between interveinal segments and veins is stronger than in Fig. 3 *D*, indicating a lower contribution of upper harmonics in veins. Using the model of a negative-feedback regulation (Eq. 12), this observation can be explained by proposing a weaker regulatory interaction δ in veins compared to interveinal segments. The second harmonic component ($\omega = 3.2\pi/60$ s^{-1}) occurred with relative amplitude roughly uniform over the leaf surface. The phase of the second harmonic component was variable with only a small positive shift in the stem and in large veins (*red*), with a significant shift of $\sim\pi/2$ in small veins (*yellow*) and a large shift approaching π in interveinal leaf segments (*green*).

Regardless of these quantitative variations, the experiment shown in Fig. 3 confirmed statistical relevance of the occurrence of the upper harmonic components in variable fluorescence during exposure of tobacco plants to harmon-

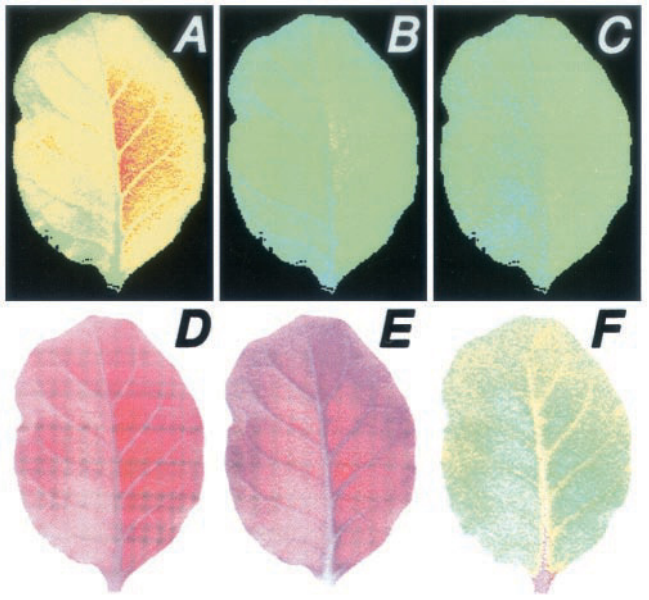

FIGURE 3 The fluorescence response of tobacco leaf exposed to harmonic irradiance of 60-s period as captured in individual pixels of the CCD camera. Images of fluorescence emission yields were captured at the maximum of the harmonic actinic light excitation F1 (*A*) and at the minimum of the actinic light excitation F0 (*B*). The rainbow false colors indicate relative intensity with red showing 185 of 256 fluorescence levels and blue showing 0 emission signal. Panel *C* shows a map of normalized variation in fluorescence yield (F1 − F0)/F1 on the scale 0-1. Panels *D–F* show results of Fourier frequency analysis of the kinetic traces of all individual pixels with the fundamental harmonic signal $\omega = 2\pi/60\ s^{-1}$ (*D*), the first upper harmonic signal $\omega = 2.2\pi/60\ s^{-1}$ (*E*), and the second upper harmonic signal $\omega = 3.2\pi/60\ s^{-1}$ (*F*). The darker the pixel, the higher the relative amplitude of the oscillation of the given frequency detected. The colors show the phase shift of a given oscillation, with red approaching the phase of the exciting light from the positive side and blue from the negative side. Green represents π, the highest difference in phase between the given harmonics and irradiance modulation. The phase shift between the second upper and the fundamental harmonic components must be considered relative to the periodicity with $2\pi/3$ of the upper harmonic component.

ically modulated irradiance. The phenomenon was further confirmed in similar experiments with several other plant species, including *Arabidopsis thaliana* (not shown).

Resonance character of the forced oscillations

Various electronic circuits or a mechanical spring are familiar systems characterized by an internal oscillation frequency Ω and by a damping constant σ (Eq. 5). When exposed to a stepwise external forcing (e.g., spring release), such systems exhibit autonomous oscillations with period Ω and damping σ (Fig. 4 *A*). When exposed to an external harmonic force such systems are rather inert as long as the external forcing occurs with frequency ω that is largely different from the internal frequency Ω. However, a dramatic increase in oscillatory amplitudes occurs when the frequency of the external forcing ω comes close to the internal frequency Ω. This behavior is predicted also for the model in Fig. 1. Equations 8 and 11 yield an amplitude of forced oscillations that depends on frequency as schematically shown in Fig. 4 *B*. Note that the period T of the autonomous oscillations in Fig. 4 *A* and the resonance frequency in Fig. 4 *B* are coupled $\omega_{RES} \approx 2\pi/T = \Omega$. The damping constant σ is reflected in the shape of the resonance peak in Fig. 4 *B*. The higher the damping in Fig. 4 *A*, the broader the resonance peak in Fig. 4 *B* appears.

Assuming that functional modules in plant photosynthesis can act as oscillators, one can predict that a similar resonance will occur in photosynthesis when the frequency of actinic irradiance comes close to an internal frequency of any of these modules ($\omega^2 \rightarrow \Omega^2 + \sigma^2 + \delta/2$ in Eq. 11). To test this hypothesis, the period of the harmonic modulation of the actinic light was varied here between 3 and 135 s and the fluorescent emission from a leaf was analyzed as a function of the modulation frequency.

Experimentally observed resonance character of the forced oscillations in plants

Fig. 5 shows the frequency response of the amplitudes (Fig. 5, *B* and *D*) and of the phases (Fig. 5 *C*) of the fundamental harmonic component (ω, *open circles*), and of the first (2ω, *triangles*) and second (3ω, *squares*) upper harmonic components in the fluorescent emission of a leaf of African violet (Fig. 5 *A*). The leaf was partially infiltrated by DCMU, the herbicide blocking the acceptor side of photosystem II. The fluorescent response of the herbicide-poisoned leaf segment to the harmonic irradiance still exhibited upper harmonics, although the frequency response of individual components (Fig. 5 *D*) is qualitatively different from the DCMU-free leaf segment (compare *B* and *D* in Fig. 5). The steady-state component q_0 (*closed circles*) in both DCMU-free (Fig. 5 *B*) and DCMU-inhibited (Fig. 5 *D*) segments is frequency-dependent. The negative feedback regulation leading to the appearance of higher harmonics and to the frequency-dependence of the steady-state fluorescence is affected, but not inhibited, by the herbicide.

Statistical relevance of the upper harmonic components in the fluorescence emission can be estimated from the signal-to-noise (S/N) ratio in the corresponding curves showing the respective amplitudes in Fig. 5, *B* and *D*. In the range of frequencies outside the resonance bands, the S/N ratio of the amplitudes was typically 28 ± 3 for the first upper harmonic component and 5 ± 1 for the second upper harmonic component (the error margins were estimated by analyzing different frequency ranges).

In the fluorescence response of the African violet we found two major resonance peaks. The very sharp resonance peak centered at $\omega_{RES-1} \approx 2\pi/59\ s^{-1}$ was found with a half-bandwidth of $\Delta_{1/2}\omega_{RES-1} \approx 2\pi(1/56 - 1/59)\ s^{-1} \approx 1/175\ s^{-1}$. A similar half-bandwidth is obtained in resonance function calculated from Eq. 11 (see Fig. 4 *B*) for a

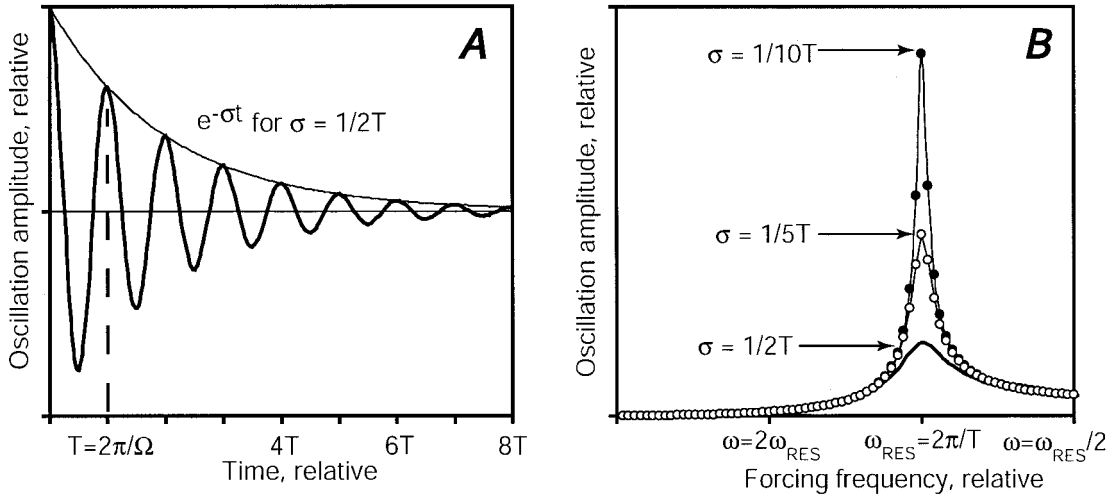

FIGURE 4 Panel *A* shows a schematic presentation of autonomous oscillations in a system described by Eq. 6 in the absence of external forcing (i.e., $a = 0$ in the scheme in Fig. 1). The system oscillates with the period $T = 2\pi/\Omega$ and the oscillations are damped with the time constant σ. The same system with zero negative-feedback regulation (i.e., $\delta = 0$ in scheme in Fig. 1) responds to an external harmonic forcing (i.e., $a \neq 0$ in scheme in Fig. 1) of angular frequency ω by oscillations of amplitude that is shown in panel *B*. The relation between the amplitude and the frequency of harmonic forcing ω was calculated from Eq. 11. The resonance occurs for a frequency of harmonic forcing ω_{RES} that is close to the frequency of autonomous oscillations $\Omega = 2\pi/T$ shown in panel *A*. The width of the resonance peak is increasing with damping constant increasing from $\sigma = 1/10T$ (*closed circles*) to $\sigma = 1/5T$ (*open circles*) and to $\sigma = 1/2T$ (*solid line*).

damping constant $\sigma \approx 1/290\ s^{-1}$. According to the relations between autonomous and forced oscillations illustrated in Fig. 4, the resonance band of the forced oscillations is expected to correspond with the occurrence of damped autonomous oscillations. Indeed, much evidence has been accumulated in earlier experiments (reviewed in Giersch, 1994; Walker, 1992) showing that autonomous photosynthetic oscillation can be induced by an abrupt change in irradiance or in CO_2 concentration, and that they usually occur with a frequency of $\sim 2\pi/60\ s^{-1}$, which is close to the resonance $\omega_{RES-1} \approx 2\pi/59\ s^{-1}$ reported here. Here, we confirmed the earlier experimental results on autonomous oscillations by exposing a leaf to a short pulse of high CO_2 administered by blowing pure gas over the leaf surface for ~1 min. Oscillations indeed occurred with a frequency of $\sim 2\pi/60\ s^{-1}$ and with a damping $\sim\sigma \approx 1/160\ s^{-1}$ (not shown). The damping was stronger than the $\sigma \approx 1/290\ s^{-1}$ predicted above from the broadening of the resonance peak. However, this apparent discrepancy is to be expected because the damping of measured autonomous oscillation is given not only by the kinetic factors reflected in the broadening of the resonance peaks, but also by mutual phase-shifts of oscillations in individual cells (Ferimazova et al., 2002).

The second resonance peak was observed in African violet centered on $\omega_{RES-2} \approx 2\pi/25\ s^{-1}$. The much larger half-bandwidth of $\Delta_{1/2}\omega_{RES-2} \approx 2\pi/5.4\ s^{-1}$ corresponded to a damping rate of $\sigma \approx 1/19\ s^{-1}$. The autonomous oscillations corresponding to this resonance band cannot occur because the damping time is shorter than the oscillation period.

The steady-state component of fluorescence (*closed circles* in Fig. 5 *B*) exhibited only a negligible variability in the range close to the sharp peak (ω_{RES-1}). The lack of resonance indicates a weak regulatory interaction δ because, according to the model (Eq. 10), the frequency-dependent fraction of the steady-state component is proportional to the square of the negative feedback interaction (δ^2). For a small interaction ($1 \gg \delta$), the resonance in the steady-state component can be negligible compared to the frequency-dependent fraction of the fundamental harmonic component that is proportional to δ (Eq. 11).

In contrast, a visible depression of the steady-state component was found in the broad resonance centered at $2\pi/25\ s^{-1}$ (*closed circles* in Fig. 5 *B*). It is predicted by the model (Eq. 10) that for a positive δ (negative feedback interaction), the frequency variation in the steady-state component has an opposite sign compared to the resonance amplitude of the first harmonic component. Indeed, the positive broad resonance peak in the amplitude of the fundamental harmonic component (*open circles* in Fig. 5 *B*, $\omega_{RES-2} \approx 2\pi/25\ s^{-1}$) correlated with a depression in the steady-state component (*closed circles* in Fig. 5 *B*). An antiparallel relation between the steady-state component and the fundamental harmonic component was also observed for the resonance peaks in the DCMU-poisoned segment of the leaf (Fig. 5 *D*).

The phase shifts of the first and second upper harmonic components (*triangles* and *squares* in Fig. 5 *C*) exhibited dramatic changes in the frequency range around the broadband resonance $\omega_{RES-2} \approx 2\pi/25\ s^{-1}$. In contrast, the fundamental harmonic component (*open circles* in Fig. 5 *C*) always remained approximately in phase with the harmonic

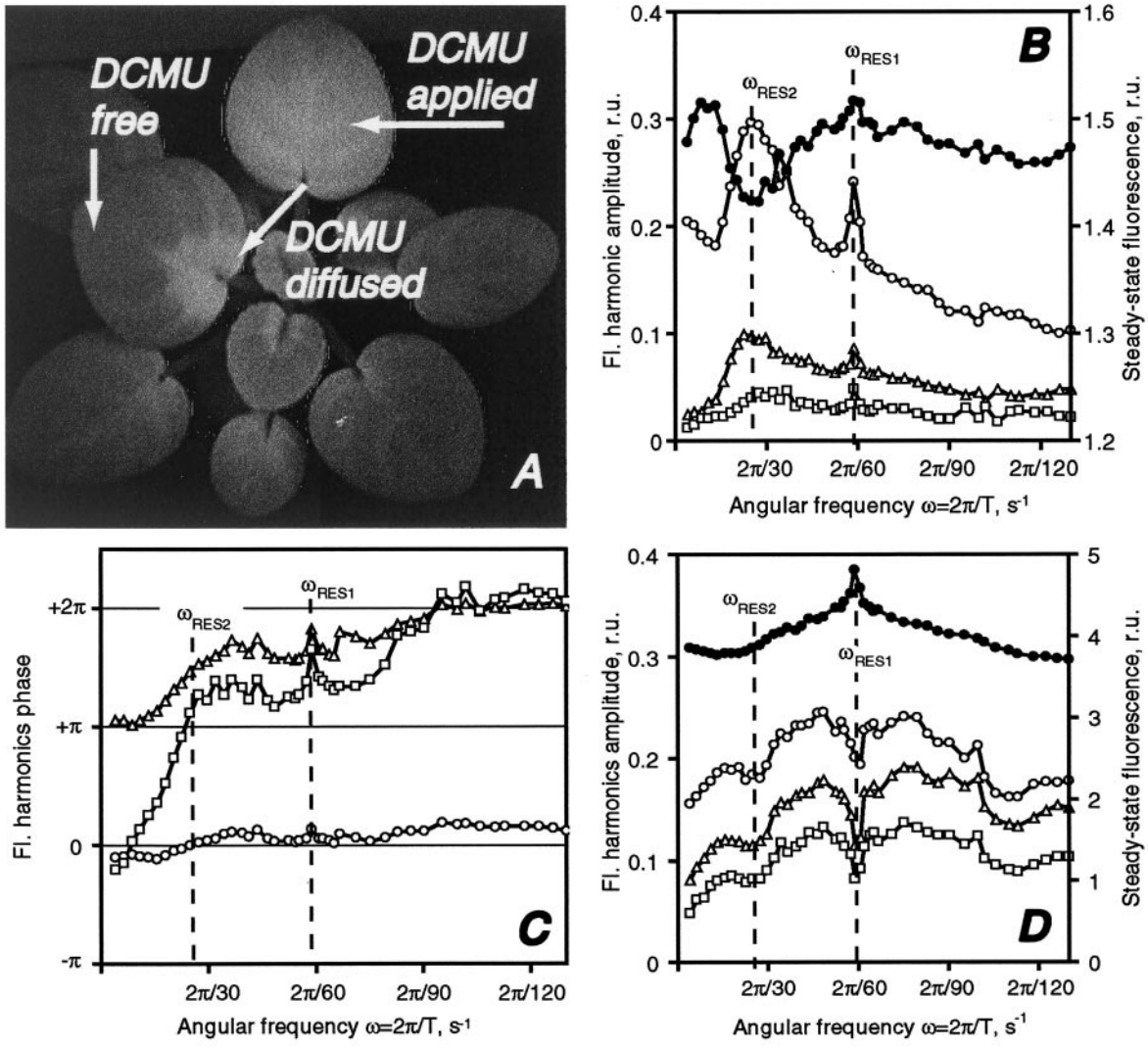

FIGURE 5 One leaf of African violet (top center in *A*, DCMU applied) was brushed with a 2 mM solution of the herbicide DCMU in 1% dimethylsulfoxide in water. After a week the herbicide was transported to a neighboring leaf, where it was localized close to the stem and large veins as visualized by elevated fluorescence emission in weak light (DCMU diffused), whereas the peripheral parts of the same leaf remained DCMU-free. The frequency response of the DCMU-free peripheral leaf segment (panels *B* and *C*) and the DCMU-inhibited segment (panel *D*) to harmonic actinic light were studied in parallel. Fluorescence transients for given frequency of harmonic irradiance were deconvoluted into a steady-state component q_0, fundamental harmonic component q_1, and two upper harmonic components q_2 and q_3 (as shown in Fig. 2, *bottom panels*). The amplitude q_0 of the steady-state fluorescence component is shown (*closed circles*) as a function of modulation frequency in panel *B* for DCMU-free and in panel *D* for DCMU-inhibited leaf segments. The frequency dependence of the amplitudes of the fundamental harmonic component (*open circles*) and of the first (*triangles*) and second (*squares*) upper harmonic components of fluorescence emission are shown in the same panels (*B* for DCMU-free and *D* for DCMU-inhibited). Individual harmonic components are phase-shifted relative to the harmonic irradiance. The phase shift of the fundamental harmonic component of fluorescence emission for DCMU-free leaf segment is shown by open circles in panel *C*. The phase shifts of the first (*triangles*) and second (*squares*) upper harmonic components are shown in panel *C*. Dominant frequencies of two resonance bands are identified by dashed lines marked ω_{RES1} and ω_{RES2}.

irradiance. Very little variability of the phase shifts was observed for all components close to the sharp resonance peak around $\omega_{RES-1} \approx 2\pi/59\ s^{-1}$.

The phase-shifts of the harmonic components were nearly constant for the leaf segment poisoned by the herbicide (not shown). The fundamental harmonic component had no phase-shift relative to harmonic irradiance; the first upper harmonic component was shifted by $\sim\pi/2$, and the second upper harmonic component was shifted by nearly π for all periods of harmonic excitation tested here (3-130 s).

The frequency analysis shown in Fig. 5 was repeated for a tobacco leaf (not shown). The sharp resonance peak $\omega_{RES-1} \approx 2\pi/59\ s^{-1}$ was even more prominent in tobacco than in African violet. The half-bandwidth was about two times narrower ($\Delta_{1/2}\omega_{RES-1} \approx 1/92\ s^{-1}$) in tobacco com-

pared to African violet. The broad band in the high-frequency range was absent in tobacco.

DISCUSSION

We propose that the occurrence of the upper harmonic components in fluorescence response of plants to harmonic irradiance is a result of a nonlinear, negative-feedback regulation of photosynthesis.

The resonance peaks found in the frequency-dependence of the harmonic amplitudes and phase-shifts (Fig. 5) are proposed to reflect dynamic properties of a component that is controlling, by a negative feedback regulation, the photosynthetic electron flow through photosystem II. In African violet leaves we found two major resonance peaks representing two different regulatory components. The resonance peak centered around $\omega_{RES-1} \approx 2\pi/59\ s^{-1}$ with a half-bandwidth $\Delta_{1/2}\omega_{RES-1} \approx 1/175\ s^{-1}$ corresponded to autonomous oscillations observed experimentally in photosynthetic activities in response to an abrupt change in air composition or in irradiance. Our estimate of the damping of such oscillations $\sigma \approx 1/290\ s^{-1}$ is much closer than the earlier models to the experimentally observed damping that extends over several oscillation periods (reviewed in Giersch, 1994; Walker, 1992). The weak damping and the narrow half-bandwidth of this resonance band is explained here by a very long intrinsic lifetime of the corresponding flux-sensing and regulatory components: $2\sigma = 1/T_1 + 1/T_1 \approx 1/145\ s^{-1}$ (Eqs. 3 and 4). The long lifetime is not compatible with a direct participation of these regulatory components in forward bioenergetic reactions that would require a damping stronger than $1.6\ s^{-1}$ reflecting the fast turnover rates (Ryde-Pettersson, 1992). More likely, the regulation is communicated through a side-chain reaction where a long response time may be an advantage to avoid an overshooting regulation.

The second resonance peak centered around $\omega_{RES-2} \approx 2\pi/25\ s^{-1}$ was much broader, with a half-bandwidth of $\Delta_{1/2}\omega_{RES-2} \approx 2\pi/5.4\ s^{-1}$ and a corresponding damping rate of $\sigma \approx \Delta_{1/2}\omega_{RES}/\sqrt{12} \approx 1/19\ s^{-1}$. The damping is so strong that the corresponding autonomous oscillations elicited by an abrupt change in irradiance or air composition cannot be observed, and the resonance can be accessed only through the forced oscillations. The absence of this peak in tobacco shows that the component responsible for the regulation may not be always active or, more likely, that the combination of the rate constants of the regulatory components prevents the resonance and the autonomous oscillations ($\Omega < 0$ in Eq. 6). The molecular nature of the regulatory mechanisms reflected in the resonance bands and in the occurrence of the upper harmonics remains obscure. Most puzzling is the persistent occurrence of the upper harmonic components and of the resonance bands in the DCMU-inhibited leaf. Irrespective of whether the inhibition is complete, the electron flow through photosystem II is substantially reduced by the herbicide, as shown by the elevated fluorescence emission in a weak light (Fig. 5 *A*) and the plastoquinone pool remains mostly oxidized during the experiment. Most likely, cyclic electron flow around photosystem I is the only process that can elicit the regulation reflected in the resonance bands and in the occurrence of the upper harmonic components in the DCMU-inhibited leaf segments.

Future system-level analysis of forced oscillations must be extended by additional variables, namely by light intensity, CO_2 concentration, and temperature. Equally relevant are the measurements of gas exchange in harmonically modulated irradiance. Our preliminary data show that the changes in irradiance do not change the central frequency of the resonance bands. This observation is in line with results presented here in Fig. 3, where the leaf was subjected to variable irradiance over its surface, and also in Fig. 5 *D*, where the effect of irradiance was modified by the herbicide.

The preliminary data also show that the upper harmonic components occur in gas exchange, although their relative amplitude is smaller than that in fluorescence. The relatively smaller resonance impact in gas exchange compared to fluorescence can be expected as a feature indicating an optimized system-level operation that is reducing effects of environment variability on the overall plant performance measured by CO_2 fixation.

The measurement of fluorescence response to harmonic irradiance reported here is a convenient tool that can facilitate further searches for the genetic and molecular basis of individual regulatory mechanisms. We predict that the upper harmonic components reflecting various regulatory modules will be found also on longer timescales that have not been covered in this study. This hypothesis is supported by the recent finding of upper harmonic components in photosynthetic activity during circadian rhythms (Bohn et al., 2001).

The technical assistance of Jiří Lisal and language correction by Steve Halperin are gratefully acknowledged.

This research was supported in part by Grant LN00A141 of the Czech Ministry of Education and by project AV0Z6087904 of the Institute of Landscape Ecology CAS. The modification of the FluorCam instrument and Recognita software were provided free of charge by P. S. Instruments, Ltd., Brno, Czech Republic.

REFERENCES

Bohn, A., A. Geist, U. Rascher, and U. Lüttge. 2001. Response to different external light rhythms by the circadian rhythm of Crassulacean acid metabolism in *Kalanchoe daigremontiana*. *Plant Cell Environ.* 24: 811–820.

Buschmann, P., and D. Gradmann. 1997. Minimal model for oscillations of membrane voltage in plant cells. *J. Theor. Biol.* 188:323–332.

Csete, M., and J. Doyle. 2002. Reverse engineering of biological complexity. *Science.* 295:1664–1669.

Demin, O., H. Westerhoff, and B. Kholodenko. 1999. Control analysis of stationary forced oscillations. *J. Phys. Chem. B.* 103:10695–10710.

Demmig-Adams, B., and W. Adams. 1992. Photoprotection and other responses of plants to high light stress. *Annu. Rev. Plant Physiol. & Plant Mol. Biol.* 43:599–626.

Dettman, J. 1961. Mathematical Methods of Physics. McGraw-Hill Book Company, New York.

Ferimazova, N., H. Kuepper, L. Nedbal, and M. Trilek. 2002. New insights into photosynthetic oscillations revealed by two-dimensional microscopic measurements of chlorophyll fluorescence kinetics in intact leaves and isolated protoplasts. *Photochem. Photobiol.* In press.

Fork, D. C., and K. Satoh. 1991. The control by state transitions of the distribution of excitation energy in photosynthesis. *Annu. Rev. Plant Physiol.* 37:335–361.

Fridlyand, L. 1998. Independent changes of ATP/ADP or ΔpH could cause oscillations in photosynthesis. *J. Theor. Biol.* 193:739–741.

Genty, B., J. M. Briantias, and N. R. Baker. 1989. The relationship between the quantum yield of photosynthetic electron transport and quenching of chlorophyll fluorescence. *Biochim. Biophys. Acta.* 990:87–92.

Giersch, C. 1994. Photosynthetic oscillations: observations and models. *Comments Theor. Biol.* 3:339–364.

Hess, B. 2000. Periodic patterns in biology. *Naturwissenschaften.* 87: 199–211.

Horton, P., and A. Ruban. 1992. Regulation of photosystem II. *Photosynth. Res.* 34:375–385.

Kitano, H. 2001. Foundations of Systems Biology. MIT Press, Cambridge.

Laisk, A., and H. Eichelmann. 1989. Towards understanding oscillations: a mathematical model of the biochemistry of photosynthesis. *Phil. Trans. R. Soc. Lond. B.* 323:369–384.

Leegood, R., T. Sharkey, and S. von Caemmerer, editors. 2000. Photosynthesis: Physiology and Metabolism. Kluwer Academic Publishers, Dordrecht/Boston/London.

Ljung, L. 1991. System Identification: Theory for the User. PTR Prentice Hall, Engelwood Cliffs, NJ.

Nedbal, L., J. Soukupová, D. Kaftan, J. Whitmarsh, and M. Trtilek. 2000. Kinetic imaging of chlorophyll fluorescence using modulated light. *Photosynth. Res.* 66:3–12.

Ort, D., and C. Yocum, editors. 1996. Oxygenic Photosynthesis: The Light Reactions. Kluwer Academic Publishers, Dordrecht/Boston/London.

Reijenga, K., H. Westerhoff, B. Kholodenko, and J. Snoep. 2002. Control analysis for autonomously oscillating biochemical networks. *Biophys. J.* 82:99–108.

Rovers, W., and C. Giersch. 1995. Photosynthetic oscillations and the interdependence of photophosphorylation and electron transport as studied by a mathematical model. *BioSystems.* 35:63–73.

Ryde-Pettersson, U. 1990. On the mechanistic origin of damped oscillations in biochemical reaction systems. *Eur. J. Biochem.* 194:431–436.

Ryde-Pettersson, U. 1992. Oscillations in the photosynthetic Calvin cycle: examination of a mathematical model. *Acta Chim. Scand.* 46:406–408.

Walker, D. 1992. Concerning oscillations. *Photosynth. Res.* 34:387–395.

Weis, E., and J. Berry. 1987. Quantum efficiency of photosystem II in relation to energy-dependent quenching of chlorophyll fluorescence. *Biochim. Biophys. Acta.* 894:198–208.